

# Photochemistry of $\text{HCl}(\text{H}_2\text{O})_4$ : Cluster Model of the Photodetachment of the Chloride Anion in Water

Andrzej L. Sobolewski\*<sup>†</sup> and Wolfgang Domcke<sup>‡</sup>

*Institute of Physics, Polish Academy of Sciences, PL-02668 Warsaw, Poland, and Institute of Physical and Theoretical Chemistry, Technical University of Munich, D-85747 Garching, Germany*

*Received: June 28, 2002; In Final Form: December 13, 2002*

The covalent, zwitterionic, and biradicalic forms of the  $\text{HCl}(\text{H}_2\text{O})_4$  cluster have been investigated with density functional theory (DFT) and time-dependent DFT (TDDFT). The equilibrium geometries and force fields of the lowest electronic states have been determined with DFT; vertical electronic excitation energies have been calculated with TDDFT. It is shown that the excited states of the  $\text{H}_3\text{O}^+(\text{H}_2\text{O})_3\text{Cl}^-$  zwitterion are of the charge-transfer-to-solvent (CTTS) type. The molecular and electronic structures of the  $\text{H}_3\text{O}(\text{H}_2\text{O})_3\text{Cl}$  biradical have been characterized for the first time. The lowest electronic states of the biradical are significantly lower in energy than the CTTS excited states of the zwitterion and therefore are photochemically accessible from the latter. The electronic and vibrational absorption spectra of the biradical are essentially identical to those of the hydrated hydronium radical,  $\text{H}_3\text{O}(\text{H}_2\text{O})_3$ , and exhibit striking similarities with the spectral signatures of the solvated electron in the liquid phase. It is argued that the photochemistry of the  $\text{H}_3\text{O}^+(\text{H}_2\text{O})_3\text{Cl}^-$  zwitterion represents a finite-size molecular model of the formation process of the solvated electron via the photodetachment of the chloride anion in water.

## 1. Introduction

The absorption spectra of halide anions in water and other polar solvents have been investigated for decades.<sup>1,2</sup> These transitions are of the charge-transfer-to-solvent (CTTS) type; that is, an electron is transferred from the p shell of the halide anion to unoccupied orbitals provided by the solvent. The CTTS spectra are structureless, Gaussian-like bands in the UV with significant oscillator strength.<sup>2</sup>

In the early investigations, the dependence of these CTTS bands on temperature and on the concentration of ionic mixtures has been considered, with the intention of obtaining information on the local solvation structure.<sup>2,3</sup> Later, the interest shifted toward the photochemistry induced by the CTTS transitions of halide anions in protic solvents. As first shown in a series of papers by Jortner, Ottolenghi, and Stein, the CTTS excited states dissociate into a halogen atom and a solvated electron. (See ref 4 and references therein.) Since then, halide anions and other anions such as ferrocyanide have served as convenient precursors for the production of solvated electrons by photodetachment. With the advent of femtosecond time-resolved laser spectroscopy, it has become possible to obtain information on individual stages of the formation and equilibration of the solvated electron in real time.<sup>5–10</sup> Quantum-classical molecular dynamics simulations have been essential for the development of a microscopic picture of the electron photodetachment and solvation processes in the liquid environment.<sup>11–14</sup>

The spectroscopy of halide anions in the liquid phase has recently been complemented by spectroscopic investigations of size-selected  $\text{X}^-$ -water clusters ( $\text{X} = \text{Cl}, \text{Br}, \text{I}$ ). CTTS absorption spectra of  $\text{I}^-(\text{H}_2\text{O})_n$  clusters have been obtained as action spectra (detection of electron detachment) for  $n = 1-4$ .<sup>15</sup>

Vibrational spectra of  $\text{X}^-(\text{H}_2\text{O})_n$  clusters with  $1 \leq n \leq 6$  have been observed in the mid-infrared via vibrational dissociation.<sup>16</sup> Real-time data on the electron solvation dynamics following the photoexcitation of  $\text{I}^-$ -water clusters have been obtained by Neumark, Weinkauff, and collaborators using femtosecond time-resolved photoelectron spectroscopy.<sup>17</sup> These spectroscopic results on size-selected anion-water clusters are obviously of relevance for the understanding of aqueous solvation at the molecular level and have stimulated a number of ab initio electronic structure calculations on the geometric structure, stability, and electronic and vibrational spectra of halide-water clusters.<sup>18–24</sup>

In the present work, we adopt a different approach toward a computational modeling of the CTTS excitation process and the formation of solvated electrons in clusters. We consider the excited electronic states and photochemical reaction mechanisms of neutral clusters of the type  $\text{HX}(\text{H}_2\text{O})_n$ , specifically,  $\text{HCl}(\text{H}_2\text{O})_4$ . The consideration of neutral clusters has the advantage of a faster convergence of spectroscopic properties with increasing cluster size since long-range monopole Coulomb potentials with their associated screening effects are absent. In liquid-phase experiments, positive counterions are generally present, at least at higher concentrations of salt solutions, and their influence may have to be considered in the interpretation of the solvation dynamics.<sup>8</sup> Overall neutral zwitterionic clusters may therefore provide more convenient finite-size models of the liquid phase than clusters with an overall negative charge.

Hydrogen chloride is known to be a very strong acid and is assumed to be fully dissociated into chloride anions and hydronium cations in the liquid phase.<sup>25,26</sup> Amirand and Maillard were the first to answer the question of how many water molecules are needed to stabilize the zwitterionic form of hydrogen chloride.<sup>27</sup> The IR spectroscopy of  $\text{HCl}$ -water clusters in a low-temperature argon matrix revealed that the  $\text{H}_3\text{O}^+(\text{H}_2\text{O})_n\text{Cl}^-$  cluster is stable for  $n \geq 3$ .<sup>27</sup> Several recent calcula-

\* Corresponding author. E-mail: sobola@ifpan.edu.pl.

<sup>†</sup> Polish Academy of Sciences.

<sup>‡</sup> Technical University of Munich.

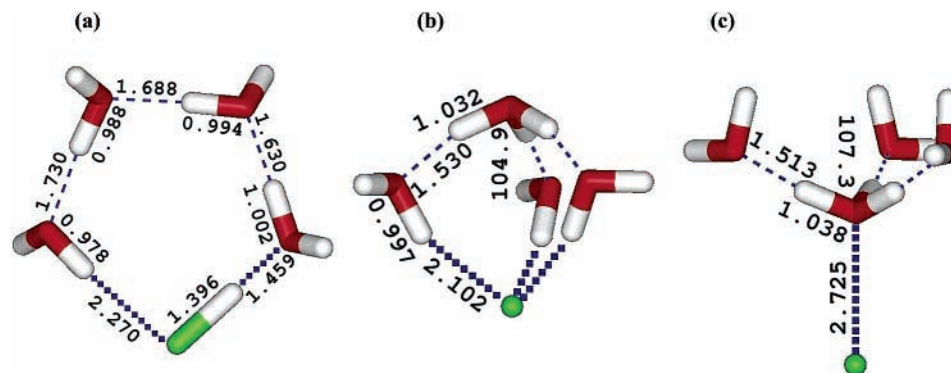


**Figure 1.** DFT/B3LYP equilibrium geometries of the electronic ground states of the (a) covalent and (b) zwitterionic forms of the  $\text{HCl}(\text{H}_2\text{O})_4$  cluster. The equilibrium geometry of the nearly degenerate  $S_1$  and  $T_1$  states of the  $\text{H}_3\text{O}(\text{H}_2\text{O})_3\text{Cl}$  biradical, obtained with the DFT/B3LYP method, is shown in c. The numbers indicate bond lengths in angstroms and HOH bond angles of the  $\text{H}_3\text{O}^+$  units (b and c) in degrees.

tions employing ab initio electronic structure theory or density functional theory (DFT) have corroborated this experimental result.<sup>28–33</sup> The  $\text{H}_3\text{O}^+(\text{H}_2\text{O})_3\text{Cl}^-$  cluster is thus the smallest neutral system that can be adopted for the investigation of the photochemistry of the chloride anion in an aqueous environment.

Calculated vertical CTTS excitation energies have been reported for several  $\text{X}^-(\text{H}_2\text{O})_n$  clusters.<sup>19–21</sup> Chen and Sheu<sup>23</sup> and Vila and Jordan<sup>24</sup> have performed limited excited-state geometry optimizations for the  $\text{I}^-(\text{H}_2\text{O})_4$  cluster. These calculations have provided information on the detachment of the electron from the iodide anion and the reorientation of the water molecules in the lowest excited state but did not reveal the reaction coordinate for the formation of the solvated electron. In the present work, we have identified the presumable reaction product versus a geometry optimization of the lowest radical-pair state of the  $\text{HCl}(\text{H}_2\text{O})_4$  cluster. The minimum-energy structure of the radical pair consists of a microsolvated hydronium radical that is loosely bound to the chlorine atom. As proposed previously,<sup>34,35</sup> the former can be identified as the carrier of the characteristic spectroscopic properties of the solvated electron.

## 2. Computational Methods

The geometries of the covalent and zwitterionic forms of the  $\text{HCl}(\text{H}_2\text{O})_4$  cluster in the electronic ground state have been determined with DFT, employing Becke's three-parameter hybrid functional containing the correlation functional of Lee, Yang, and Parr (B3LYP). The stability of the stationary points has been confirmed by vibrational analysis. IR spectra have been calculated in the harmonic approximation. The energies of the DFT-optimized minimum structures have also been determined by single-point calculations with the second-order Møller–Plesset (MP2) method.

Direct unconstrained geometry optimization of the CTTS excited singlet states of the cluster is not possible because of the variational collapse of the electronic wave function to the electronic ground state. Anticipating that the energy minimum must correspond to a biradicalic structure, for which the singlet–triplet splitting is negligibly small, we can instead optimize the energy of the lowest triplet state of the cluster. Once the geometric structure of the biradical has been found, it is straightforward to compute the singlet energy spectrum at this geometry.

The standard 6-31+G\*\* split-valence double- $\zeta$  Gaussian basis set augmented with polarization functions on all atoms and diffuse functions on the heavy atoms<sup>36</sup> has been employed. Anticipating that the biradical possesses Rydberg character (see below), the basis set was supplemented with an additional set

of diffuse s and p Gaussian functions of exponent  $\zeta = 0.02$  on the oxygens, drawing on previous experience obtained for  $\text{H}_3\text{O}^-$  water clusters.<sup>35</sup> This basis set consisting of 267 Gaussian primitives was used in the geometry optimizations and in the calculation of vibrational spectra as well as in the MP2 energy calculations. The spin–orbit splitting of the chlorine radical is ignored in these nonrelativistic calculations.

For the calculation of the electronic excitation spectrum at the optimized geometries, the time-dependent DFT (TDDFT) method has been used with the B3LYP functional. To obtain a better description of higher excited states with more pronounced Rydberg character, additional diffuse s and p Gaussian functions with an exponent of  $\zeta = 0.005$  have been added on the oxygen atoms. This basis set consists of 287 Gaussian primitives.

All calculations have been performed with the Gaussian 98 program package.<sup>37</sup>

## 3. Results and Discussion

**A. Geometric and Electronic Structures.** The molecular structures of the covalent (that is, non-ion-pair-dissociated) and zwitterionic forms of the  $\text{HCl}(\text{H}_2\text{O})_4$  cluster, optimized at the DFT/B3LYP level as described above, are shown in Figure 1a and b, respectively. These structures have been determined previously by several workers using Hartree–Fock, MP2, and DFT methods.<sup>28–33</sup> The covalent form is a cyclic pentamer with a very short (1.459 Å) hydrogen bond between the H atom of HCl and the neighboring water molecule and an elongated (1.396 Å) HCl bond length. The present geometry parameters for  $\text{HCl}(\text{H}_2\text{O})_4$  agree within about 0.01 Å with those of ref 33, where the DFT/B3LYP method with a somewhat larger basis set (aug-cc-pVDZ, 364 primitive Gaussians) has been employed. The zwitterionic form of  $\text{HCl}(\text{H}_2\text{O})_4$  is a trigonal bipyramid consisting of a hydronium cation and a chloride anion that are separated by a layer of three water molecules; see Figure 1b. This structure is remarkably compact, with very short (1.530 Å) hydrogen bonds between  $\text{H}_3\text{O}^+$  and the three water molecules. The present geometry parameters are again in agreement within 0.01–0.02 Å with those reported in ref 33.

At the DFT/B3LYP level with the present basis set, the zwitterionic form is more stable by 0.112 eV (2.58 kcal/mol) than the covalent form. The MP2 energies calculated at the DFT/B3LYP optimized geometries yield an energy difference of merely 0.5 kcal/mol. The DFT/B3LYP energy difference is in amazingly good agreement with the value of 2.43 kcal/mol obtained with CCSD(T) calculations at DFT/B3LYP optimized geometries.<sup>33</sup> When zero-point energy corrections are included at the DFT/B3LYP level, the zwitterionic form is found to be below the covalent form by only 0.1 kcal/mol, in close

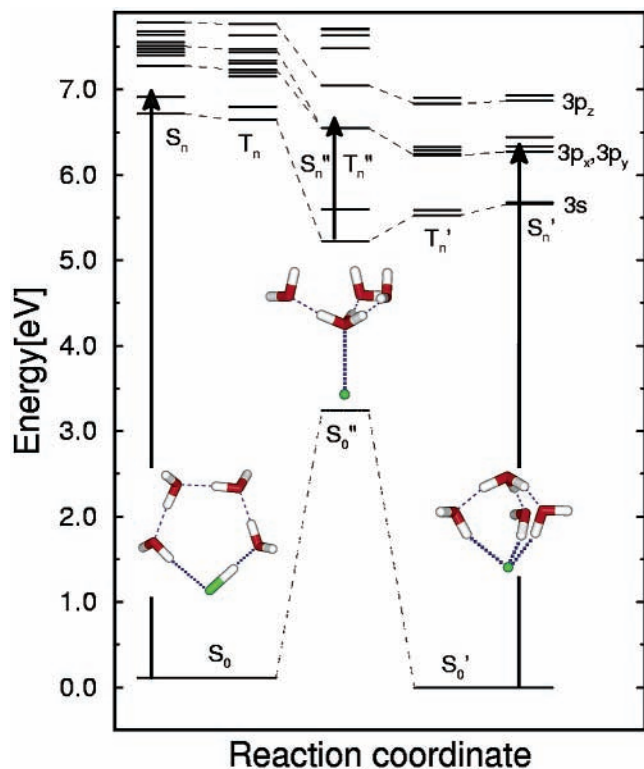


**Figure 2.** Energy diagram of the ground states and vertically excited states of the covalent ( $S_n$ ,  $T_n$ ), biradical ( $S_n''$ ,  $T_n''$ ), and zwitterionic ( $S_n'$ ,  $T_n'$ ) forms of the  $\text{HCl}(\text{H}_2\text{O})_4$  cluster. For the biradical, the  $S_n''$  and  $T_n''$  ( $n > 0$ ) states are essentially degenerate. The arrows schematically indicate the electronic transitions pertaining to the absorption spectra shown in Figure 3. Dashed lines correlate the 3s and 3p Rydberg levels of water populated with an electron excited from the 3s orbital of chlorine.

agreement with the value of 0.7 kcal/mol reported in ref 30. The calculations thus consistently predict that the covalent and ion-pair forms of the  $\text{HCl}(\text{H}_2\text{O})_4$  cluster are essentially isoenergetic.

A new result of the present work is the molecular structure of the biradical form of the  $\text{HCl}(\text{H}_2\text{O})_4$  cluster shown in Figure 1c. As discussed in section 2, this structure has been found by an unconstrained optimization of the energy of the lowest triplet state. The biradical exhibits trigonal symmetry like the zwitterion, but the umbrella angle of the hydronium cation is inverted, and the water shell is now located on the opposite side of the chlorine atom. The biradical is obtained from the zwitterion by the transfer of an electron from the chloride anion to the microsolvated  $\text{H}_3\text{O}^+$  unit, forming a microsolvated  $\text{H}_3\text{O}$  radical. The bond lengths of the hydrogen bonds in the radical are even shorter (1.513 Å) than those in the zwitterion. The rather long O–Cl distance of 2.725 Å indicates a loose binding of the  $\text{H}_3\text{O}(\text{H}_2\text{O})_3$  radical with the Cl radical.

The calculated energies (relative to the ground-state energy of the zwitterionic cluster) of the structures discussed so far as well as the corresponding vertical excitation energies (calculated with TDDFT) are shown in Figure 2. Singlet and triplet excited states are included for the covalent and zwitterionic forms, denoted as  $S_n$ ,  $T_n$  and  $S_n'$ ,  $T_n'$ , respectively. For the biradical, singlet and triplet excited states are essentially degenerate, and we denoted them as  $S_n''$ ,  $T_n''$ . The level designated  $S_0''$  represents the singlet ground-state energy calculated at the geometry of the biradical (Figure 1c). The lowest biradical singlet state is  $S_1''$ , quasidegenerate with  $T_1''$ , for which the energy has been optimized. The vertical arrows in Figure 2

indicate schematically the transitions corresponding to the electronic spectra of the three species. As will be discussed in more detail below, the excitation energies of the zwitterion and the covalent cluster are located in the far UV, around 6–7 eV. The excitation energies of the biradical cluster, however, are very low; see Figure 2. The excitation energy of the lowest strongly allowed optical transition, indicated by the arrow in Figure 2, is below 2 eV. It is also seen in Figure 2 that the  $S_1''$  energy level of the biradical is lower than the  $S_1$  and  $S_1'$  energy levels of the covalent cluster and the zwitterion, respectively. The biradical can thus be formed by an exothermic relaxation process after optical excitation of either the covalent or zwitterionic forms of the cluster.

To provide insight into the electronic structure of the three species, we display in Figure 3 the highest occupied orbitals (HOMO) and lowest unoccupied orbitals (LUMO) of the covalent cluster (a, b) and the zwitterion (c, d), as well as the two singly occupied orbitals (SOMO) of the zwitterion (e, f). These orbitals have been obtained by restricted Hartree–Fock (RHF) calculations for the  $S_0$  and  $T_1$  states, respectively, at the respective geometries.

The HOMO and the LUMO of the covalent cluster (Figure 3a and b) show the character of the lowest-energy electronic transition: an electron is excited from the p shell of the chlorine atom to a Rydberg-like  $\sigma^*$  orbital mostly localized on the HCl and the neighboring water molecules. The  $\sigma^*$  orbital is seen to be antibonding with respect to both the covalent bond of HCl and the HCl– $\text{H}_2\text{O}$  hydrogen bond, indicating that the cyclic structure will be unstable in the  $p\sigma^*$  excited state.

The HOMO and LUMO of the zwitterion in Figure 3c and d illustrate the expected CTTS character of the excited state in this case. The HOMO  $\rightarrow$  LUMO excitation corresponds to the transfer of an electron from the p shell of the chloride anion to a diffuse Rydberg orbital that is delocalized over all three water molecules of the first solvation shell of  $\text{Cl}^-$  and  $\text{H}_3\text{O}^+$ . The hole in the  $\sigma^*$  orbital caused by Pauli repulsion with the valence electrons of  $\text{Cl}^-$  is clearly visible.

Finally, Figure 3e and f display the SOMOs of the biradical, a  $p_z$ -type orbital, on the chlorine atom and a  $\sigma^*$  orbital, which is stabilized by the hydronium cation and three solvating water molecules. It can be clearly seen that the overlap of the p orbital on the loosely bound chlorine atom and the  $\sigma^*$  orbital on the other side of the  $\text{H}_3\text{O}^+(\text{H}_2\text{O})_3$  crown is essentially zero, explaining the quasi-degeneracy of the singlet and triplet states of the biradical. The  $\sigma^*$  orbital in Figure 3f is very similar to that obtained previously for the microsolvated hydronium radical  $\text{H}_3\text{O}(\text{H}_2\text{O})_3$ .<sup>34</sup> The low-lying  $S_n''/T_n''$  excited states in Figure 2 correspond to excitations from the 3s-type Rydberg orbital of Figure 3f to higher (3p, etc.) Rydberg orbitals of water.

**B. Electronic and Vibrational Spectra.** Figure 4 gives the energies (vertical excitation energies) and intensities (oscillator strengths) of the electronic transitions of the three  $\text{HCl}(\text{H}_2\text{O})_4$  species considered in this work, obtained with the TDDFT method. The electronic absorption spectrum of the cyclic  $\text{HCl}(\text{H}_2\text{O})_4$  cluster is located in the far UV, above 6.5 eV (Figure 4a). Since we are not aware of any experimental data on the electronic spectroscopy of this cluster, we skip a detailed discussion of this spectrum.

The electronic absorption spectrum of the zwitterion is located above 5.7 eV; see Figure 4b. The thick lines in Figure 4b represent degenerate ( $^1\text{E}$ ) excited states. (Their intensity has to be multiplied by a factor of 2.) The thin lines represent nondegenerate ( $^1\text{A}$ ) excited states. We have calculated 20 excited

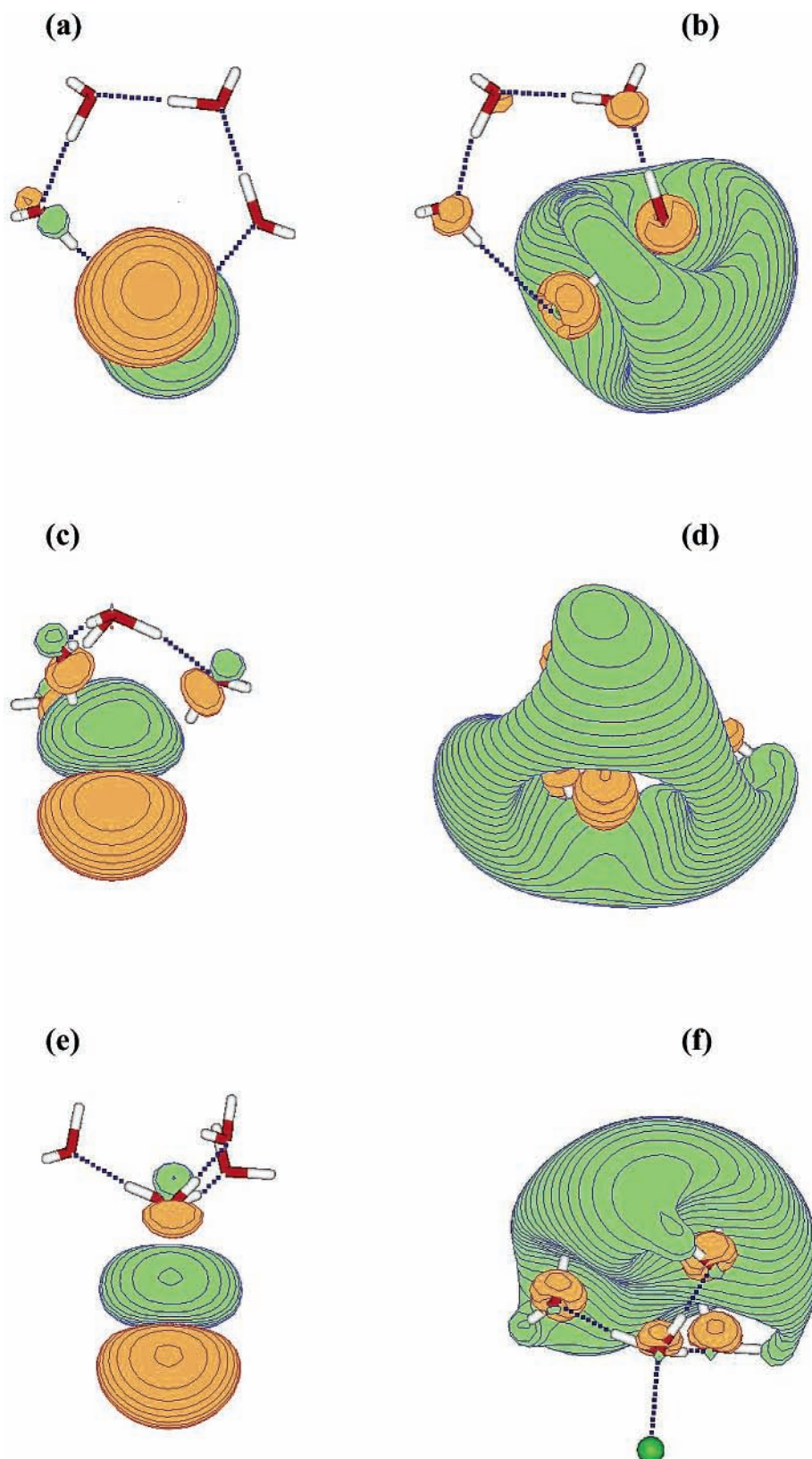


**Figure 3.** (a, c) HOMO and (b, d) LUMO of the covalent and zwitterionic forms of the  $\text{HCl}(\text{H}_2\text{O})_4$  cluster, respectively, obtained by RHF calculations at the respective equilibrium geometries. (e) and (f) display the singly occupied orbitals of the biradical obtained by a UHF calculation for the  $T_1$  state at the equilibrium geometry of the biradical.

singlet states that cover an energy range up to 7 eV. The sum of the oscillator strengths of the transitions is 0.24, in qualitative agreement with experimental estimates of the oscillator strength of CTTS transitions of halide anions in water.<sup>2</sup> The peak position of the CTTS spectrum of  $\text{Cl}^-$  in liquid  $\text{H}_2\text{O}$  has been reported

to be 6.76 eV<sup>2</sup> and 7.10 eV.<sup>38</sup> It is to be expected that the CTTS spectrum in the liquid is blue-shifted relative to the spectrum of small clusters since the diffuse  $\sigma^*$  orbital (cf. Figure 3d) will be compressed by the liquid environment. Apart from this effect, the spectrum calculated for the  $\text{Cl}^-(\text{H}_2\text{O})_3\text{H}_3\text{O}^+$  cluster seems

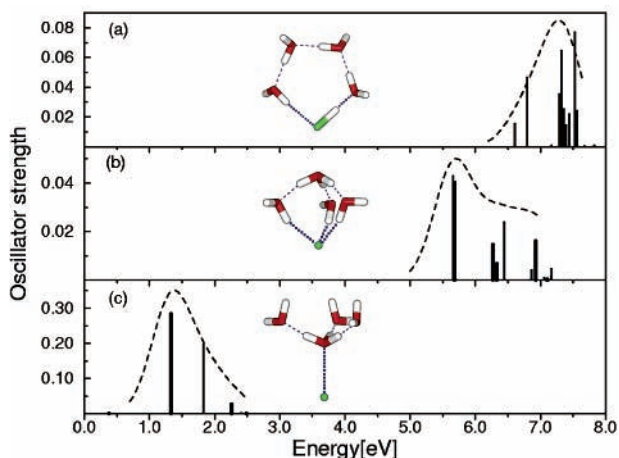


**Figure 4.** Vertical electronic excitation spectra of the (a) covalent, (b) zwitterionic, and (c) biradical forms of the  $\text{HCl}(\text{H}_2\text{O})_4$  cluster calculated with the TDDFT/B3LYP method. Bold, vertical bars denote transitions to degenerate ( $E$  symmetry) excited states. Dashed curves were obtained by broadening the calculated bars, assuming Gaussian functions of 0.7 eV halfwidth.

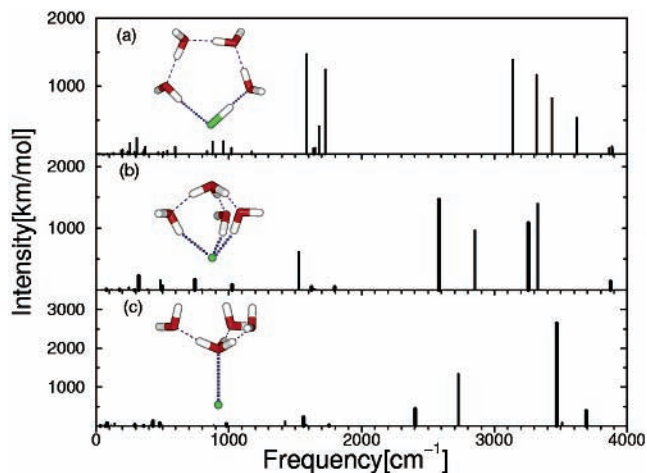
to provide a good description of the CTTS absorption band of the chloride anion in water.

Figure 4c shows the electronic absorption spectrum of the  $\text{H}_3\text{O}(\text{H}_2\text{O})_3\text{Cl}$  biradical. Again, thick lines denote transitions to degenerate electronic states. (Their intensities have to be multiplied by a factor of 2.) The spectrum is dominated by two intense transitions in the near infrared/visible region. The spectrum of the biradical in Figure 4c is essentially identical to that calculated previously (at the CASPT2 level) for the  $\text{H}_3\text{O}(\text{H}_2\text{O})_3$  radical.<sup>34,35</sup> The absorption spectrum of  $\text{H}_3\text{O}(\text{H}_2\text{O})_3\text{Cl}$  is thus completely dominated by the hydronium part of the biradical, which is negligibly perturbed by the Cl atom. Among 20 states calculated up to 3 eV, the two intense lines near 1.3 and 1.8 eV are associated with the transition from the  $3s$ -like ground state of the hydronium radical to the  $3p_{x,y}$  and  $3p_z$  orbitals, respectively. The sum of the oscillator strengths of transitions between 1 and 3 eV is 0.85.

As can be seen in Figure 2, there also exists an electronic transition at very low energy, 0.38 eV, in the biradical. This transition has a very small oscillator strength and is therefore hardly visible in the spectrum of Figure 4c. This line corresponds to an internal  $3p_z \rightarrow 3p_{x,y}$  excitation of the chlorine atom.

It has been pointed out previously that the  $3s \rightarrow 3p$  transition of  $\text{H}_3\text{O}$  falls into the energy range of the absorption spectrum of the hydrated electron.<sup>39–41</sup> More recently, the absorption spectra of microsolvated hydronium radicals up to  $\text{H}_3\text{O}(\text{H}_2\text{O})_9$  have been calculated, and it has been shown that the spectra of these clusters cover roughly the energy range of the absorption spectrum of the hydrated electron in the liquid phase.<sup>34,35</sup> These findings support the identification of the electronic spectrum of the  $\text{H}_3\text{O}(\text{H}_2\text{O})_3\text{Cl}$  biradical with that of the solvated electron in the bulk. We therefore propose that the CTTS excitation of the  $\text{Cl}^-(\text{H}_2\text{O})_3\text{H}_3\text{O}^+$  zwitterion and the subsequent rearrangement to the  $\text{Cl}(\text{H}_2\text{O})_3\text{H}_3\text{O}$  biradical represent the basic molecular aspects of the generation of solvated electrons in water via the photodetachment of chloride anions.

The vibrational spectra of the three  $\text{HCl}(\text{H}_2\text{O})_4$  species obtained in the harmonic approximation with the DFT/B3LYP method are shown in Figure 5. The systems with trigonal symmetry (the zwitterion, Figure 5b and the biradical, Figure



**Figure 5.** Vibrational spectra of the (a) covalent, (b) zwitterionic, and (c) biradical forms of the  $\text{HCl}(\text{H}_2\text{O})_4$  clusters calculated in the harmonic approximation at the DFT/B3LYP level. Bold, vertical bars denote transitions for degenerate ( $E$  symmetry) vibrational levels.

5c) possess degenerate vibrational levels ( $E$  symmetry), which are indicated by thick bars. The corresponding intensities have to be multiplied by a factor of 2. Thin bars denote nondegenerate vibrational levels ( $A$  symmetry). The IR spectra of the covalent and zwitterionic forms of  $\text{HCl}(\text{H}_2\text{O})_4$  have been obtained previously by Re et al.<sup>30</sup> and Bacelo et al.<sup>32</sup> with similar methods and results. These spectra are included here for comparison with the vibrational spectrum of the biradical, calculated for the first time in the present work.

In the covalent cluster (Figure 5a), all OH stretching vibrations are located above  $3000\text{ cm}^{-1}$ . The lines in the  $1500\text{--}1800\text{ cm}^{-1}$  range are associated with HOH bending whereas the vibrations below  $1000\text{ cm}^{-1}$  are librations and ring deformations. The intense line at  $1588\text{ cm}^{-1}$  in Figure 5a represents the HCl stretching vibration of the cyclic cluster. The strong lines at  $3257$  and  $3325\text{ cm}^{-1}$  in the spectrum of the zwitterion (Figure 5b) are the stretching vibrations of the OH groups solvating the  $\text{Cl}^-$  anion. The degenerate vibration at  $2584\text{ cm}^{-1}$  and the nondegenerate vibration at  $2854\text{ cm}^{-1}$ , both of which are very intense, are assigned as the asymmetric and symmetric stretching vibration of the hydronium cation, respectively. The remaining prominent line at  $1525\text{ cm}^{-1}$  represents the umbrella vibration of  $\text{H}_3\text{O}^+$ .

The IR spectrum of the biradical (Figure 5c) exhibits a very intense (nearly  $6000\text{ km/mol}$ ) OH asymmetric stretching band at  $3469\text{ cm}^{-1}$ . This is the stretching vibration of the terminal OH groups that solvate the localized electron cloud confined by the  $\text{H}_3\text{O}^+(\text{H}_2\text{O})_3$  crown (cf. Figure 3f). The somewhat less intense thick line at  $2405\text{ cm}^{-1}$  and the thin line at  $2730\text{ cm}^{-1}$  represent the asymmetric and symmetric stretching vibrations, respectively, of the central  $\text{H}_3\text{O}^+$  unit of the biradical.

As found above for the electronic spectrum, the IR spectrum of the  $\text{H}_3\text{O}(\text{H}_2\text{O})_3\text{Cl}$  biradical is essentially identical to that obtained previously (with the same computational methods) for the  $\text{H}_3\text{O}(\text{H}_2\text{O})_3$  radical.<sup>34</sup> The loosely bound Cl atom does not noticeably perturb the IR absorption spectrum, which is dominated by the OH stretching vibrations of  $\text{H}_3\text{O}^+$  and the terminal water molecules. The very intense OH stretching lines associated with the OH groups pointing toward the electron cloud have been detected by Johnson and collaborators in  $\text{X}^-(\text{H}_2\text{O})_n$  clusters as well as in negatively charged water clusters.<sup>16,42,43</sup>

#### 4. Conclusions

We have analyzed in this work the molecular and electronic structures of the  $\text{H}_3\text{O}(\text{H}_2\text{O})_3\text{Cl}$  biradical. It has been shown that the biradical represents a well-defined local minimum of the potential-energy surface of the lowest triplet state ( $T_1$ ) of the  $\text{HCl}(\text{H}_2\text{O})_4$  cluster. For technical reasons, the  $T_1$  rather than the  $S_1$  energy has been minimized to obtain the geometry of the biradical. The  $S_n$  and  $T_n$  states of the biradical are essentially degenerate because of the clear spatial separation of the unpaired electrons. The energy of the biradical in its lowest electronic state ( $S_1$  or  $T_1$ ) is found to lie significantly below the vertically excited  $S_1$  states of the covalent and zwitterionic structures. The biradical can thus be formed by a relaxation process after electronic excitation of the closed-shell species, in particular, after CTTS excitation of the zwitterion. It has been shown that both the electronic absorption spectrum and the vibrational spectrum of the  $\text{H}_3\text{O}(\text{H}_2\text{O})_3\text{Cl}$  biradical are essentially identical to that of the hydrated hydronium radical,  $\text{H}_3\text{O}(\text{H}_2\text{O})_3$ .

It is suggested on the basis of the above computational results that the photochemistry of the  $\text{Cl}^-(\text{H}_2\text{O})_3\text{H}_3\text{O}^+$  zwitterion can be considered to be a finite-size molecular model of the formation of the solvated electron by the photodetachment of the chloride anion in water. The cluster models discussed so far<sup>34,44,45</sup> explain how one and the same species, namely, the hydrated hydronium radical, can be produced in three seemingly different ways, namely, by the near-threshold photoexcitation of neat water,<sup>34</sup> by the photoexcitation of organic chromophores such as indole or phenol in water,<sup>44,45</sup> and by the photodetachment of halide anions in water (this work). Preliminary calculations<sup>46</sup> for cluster models of salt solutions ( $\text{LiCl}(\text{H}_2\text{O})_4$ ,  $\text{NaCl}(\text{H}_2\text{O})_4$ , etc.) indicate that a very similar picture to that discussed here for  $\text{HCl}(\text{H}_2\text{O})_4$  emerges for these species. Taken together, these computational studies provide increasingly compelling evidence for the association of the well-known absorption spectrum of the hydrated electron<sup>47</sup> with the electronic absorption spectrum of the hydrated hydronium radical or, more generally, with a hydrated metal radical ( $M_{\text{aq}}$ ) composed of a solvated electron and a cation,  $M^+ = \text{H}^+$ ,  $\text{Li}^+$ ,  $\text{Na}^+$  and so forth, incorporated into the water network. Apparently, the spectroscopic properties of the solvated radicals are only weakly dependent on the cation and thus reflect the properties of a Rydberg electron in water.

A substantiation of the connection of the spectroscopy of  $\text{H}_3\text{O}(\text{H}_2\text{O})_n\text{X}$  biradicals with the spectroscopy of the solvated electron in liquid water requires additional calculations for larger clusters. For the hydrated hydronium radical,  $\text{H}_3\text{O}(\text{H}_2\text{O})_{3m}$ , it has been demonstrated that the localized electron cloud separates from the  $\text{H}_3\text{O}^+$  cation with increasing cluster size at zero temperature.<sup>35</sup> It is noteworthy, however, that the convergence of the spectroscopic properties with cluster size is much faster for these neutral radical clusters than for charged clusters such as  $\text{X}^-(\text{H}_2\text{O})_n$  or  $(\text{H}_2\text{O})_n^-$ . Apart from the effects of thermal fluctuations, the spectra of radical defects in water can thus efficiently be studied by ab initio calculations for relatively small clusters.

**Acknowledgment.** This work has been supported by the Deutsche Forschungsgemeinschaft through SFB 377 and the Committee for Scientific Research of Poland (grant no. 3 T09A 082 19).

#### References and Notes

- (1) Rabinowitch, E. *Rev. Mod. Phys.* **1942**, *14*, 112.
- (2) Blandamer, M. J.; Fox, M. F. *Chem. Rev.* **1970**, *70*, 59.

- (3) Stein, G.; Treinin, A. *Trans. Faraday Soc.* **1960**, *56*, 1393.
- (4) Jortner, J.; Ottolenghi, M.; Stein, G. *J. Phys. Chem.* **1964**, *68*, 247.
- (5) Long, F. H.; Lu, H.; Eisenthal, K. B. *J. Chem. Phys.* **1989**, *91*, 4413.
- (6) Long, F. H.; Lu, H.; Eisenthal, K. B. *Chem. Phys. Lett.* **1990**, *169*, 165.
- (7) Gauduel, Y.; Gelabert, H.; Ashokkumar, M. *Chem. Phys.* **1995**, *197*, 167.
- (8) Gauduel, Y.; Gelabert, H. *Chem. Phys.* **2000**, *256*, 333.
- (9) Assel, M.; Laenen, R.; Laubereau, A. *Chem. Phys. Lett.* **1998**, *289*, 267.
- (10) Vilchiz, V. H.; Kloepfer, J. A.; Germaine, A. C.; Lenchenkov, V. A.; Bradforth, S. E. *J. Phys. Chem. A* **2001**, *105*, 1711.
- (11) Sheu, W. S.; Rosicky, P. J. *J. Chem. Phys. Lett.* **1993**, *202*, 186.
- (12) Sheu, W. S.; Rosicky, P. J. *J. Phys. Chem.* **1996**, *100*, 1295.
- (13) Borgis, D.; Staib, A. *Chem. Phys. Lett.* **1994**, *230*, 405.
- (14) Staib, A.; Borgis, D. *J. Chem. Phys.* **1996**, *104*, 9027.
- (15) Serxner, D.; Dessent, C. E. H.; Johnson, M. A. *J. Chem. Phys.* **1996**, *105*, 7231.
- (16) Ayotte, P.; Bailey, C. G.; Weddle, G. H.; Johnson, M. A. *J. Phys. Chem. A* **1998**, *102*, 3067.
- (17) Lehr, L.; Zanni, M. T.; Frischkorn, C.; Weinkauff, R.; Neumark, D. M. *Science (Washington, D.C.)* **1999**, *284*, 635.
- (18) Cabarcos, O. M.; Weinheimer, C. J.; Lisy, J. M.; Xantheas, S. S. *J. Chem. Phys.* **1999**, *110*, 5.
- (19) Majumdar, D.; Kim, J.; Kim, K. S. *J. Chem. Phys.* **2000**, *112*, 101.
- (20) Kim, J.; Lee, H. M.; Suh, S. B.; Majumdar, D.; Kim, K. S. *J. Chem. Phys.* **2000**, *103*, 5259.
- (21) Chen, H. Y.; Sheu, W.-S. *J. Am. Chem. Soc.* **2000**, *122*, 7534.
- (22) Lee, H. M.; Kim, K. S. *J. Chem. Phys.* **2001**, *114*, 4461.
- (23) Chen, H.-Y.; Sheu, W.-S. *Chem. Phys. Lett.* **2001**, *335*, 475.
- (24) Vila, F. D.; Jordan, K. D. *J. Phys. Chem. A* **2002**, *106*, 1391.
- (25) Laasonen, K. E.; Klein, M. L. *J. Phys. Chem. A* **1997**, *101*, 98.
- (26) Ando, K.; Hynes, J. T. *J. Phys. Chem. B* **1997**, *101*, 10464.
- (27) Amirand, C.; Maillard, D. *J. Mol. Struct.* **1988**, *176*, 181.
- (28) Lee, C.; Sosa, C.; Planas, M.; Novoa, J. J. *J. Chem. Phys.* **1996**, *104*, 7081.
- (29) Planas, M.; Lee, C.; Novoa, J. J. *J. Phys. Chem.* **1996**, *100*, 16495.
- (30) Re., S.; Osamura, Y.; Suzuki, Y.; Schaefer, H. F., III. *J. Chem. Phys.* **1998**, *109*, 973.
- (31) Smith, A.; Vincent, M. A.; Hillier, I. H. *J. Phys. Chem. A* **1999**, *103*, 1132.
- (32) Babelo, D. E.; Binning, R. C., Jr.; Ishikawa, Y. *J. Phys. Chem. A* **1999**, *103*, 4631.
- (33) Milet, A.; Struniewicz, C.; Moszynski, R.; Wormer, P. E. *J. Chem. Phys.* **2001**, *115*, 349.
- (34) Sobolewski, A. L.; Domcke, W. *Phys. Chem. Chem. Phys.* **2002**, *4*, 4.
- (35) Sobolewski, A. L.; Domcke, W. *J. Phys. Chem. A* **2002**, *106*, 4158.
- (36) Gordon, M. S.; Binkley, J. S.; Pople, J. A.; Pietro, W. Z.; Hehre, W. J. *J. Am. Chem. Soc.* **1982**, *104*, 2797.
- (37) Frisch, M. J.; Trucks, G. W.; Schlegel, H. B.; Scuseria, G. E.; Robb, M. A.; Cheeseman, J. R.; Zakrzewski, V. G.; Montgomery, J. A., Jr.; Stratmann, R. E.; Burant, J. C.; Dapprich, S.; Millam, J. M.; Daniels, A. D.; Kudin, K. N.; Strain, M. C.; Farkas, O.; Tomasi, J.; Barone, V.; Cossi, M.; Cammi, R.; Mennucci, B.; Pomelli, C.; Adamo, C.; Clifford, S.; Ochterski, J.; Petersson, G. A.; Ayala, P. Y.; Cui, Q.; Morokuma, K.; Malick, D. K.; Rabuck, A. D.; Raghavachari, K.; Foresman, J. B.; Cioslowski, J.; Ortiz, J. V.; Stefanov, B. B.; Liu, G.; Liashenko, A.; Piskorz, P.; Komaromi, I.; Gomperts, R.; Martin, R. L.; Fox, D. J.; Keith, T.; Al-Laham, M. A.; Peng, C. Y.; Nanayakkara, A.; Gonzalez, C.; Challacombe, M.; Gill, P. M. W.; Johnson, B. G.; Chen, W.; Wong, M. W.; Andres, J. L.; Head-Gordon, M.; Replogle, E. S.; Pople, J. A. *Gaussian 98*; Gaussian, Inc.: Pittsburgh, PA, 1998.
- (38) Fox, M. F.; Barker, B. E.; Hayon, E. *J. Chem. Soc., Faraday Trans. 1* **1978**, *74*, 1776.
- (39) Schwartz, M. E. *Chem. Phys. Lett.* **1976**, *40*, 1.
- (40) Hameka, H. F.; Robinson, G. W.; Marsden, C. J. *J. Phys. Chem.* **1987**, *91*, 3150.
- (41) Muguet, F. F.; Gelabert, H.; Gauduel, Y. *J. Chim. Phys.* **1996**, *93*, 1808.
- (42) Bailey, C. G.; Kim, J.; Johnson, M. A. *J. Phys. Chem.* **1996**, *100*, 16782.
- (43) Ayotte, P.; Bailey, C. G.; Kim, J.; Johnson, M. A. *J. Chem. Phys.* **1998**, *108*, 444.
- (44) Sobolewski, A. L.; Domcke, W. *Chem. Phys. Lett.* **2000**, *329*, 130.
- (45) Sobolewski, A. L.; Domcke, W. *J. Phys. Chem. A* **2001**, *105*, 9275.
- (46) Sobolewski, A. L.; Domcke, W. To be submitted for publication.
- (47) Hart, E. J.; Boag, J. W. *J. Am. Chem. Soc.* **1962**, *84*, 4090.